Mem. S.A.It. Vol. 80, 157

Memorie della

Why galaxies care about Asymptotic Giant Branch Stars

S. Cristallo[1], O. Straniero[1], R. Gallino[2,3], L. Piersanti[1], I. Domínguez[3], and M.T. Lederer[4]

[1] INAF - Osservatorio Astronomico di Collurania, via M. Maggini, 64100 Teramo, Italy
[2] Dipartimento di Fisica Generale, Università di Torino, via P. Giuria 1, 10125 Torino, Italy
[3] Center for Stellar and Planetary Astrophysics, School of Mathematical Sciences, Monash University, PO Box 28, Victoria 3800 Australia
[4] Departimento Fisica Teorica y del Cosmos, Universidad de Granada, 18071 Granada, Spain
[5] Institut für Astronomie, Türkenschanzstraße 17, A-1180 Wien, Austria

Abstract. In the last 30 years much efforts have been devoted in modelling the longest phases characterizing the life of a star, i.e. core hydrogen burning and core helium burning. In the past, final phases of stellar evolution such as SuperNovae (SNe) phenomena (massive stars) or Asymptotic Giant Branch (AGB) (intermediate and low mass stars), have been quite often approached with oversimplified theories, due to evident difficulties in understanding and treating the involved physics. While SNe are fundamental tools for a correct comprehension of the expansion history of the Universe, AGB stars are as much precious objects for several reasons. Thanks to their very large luminosities, these stars are excellent tracers of halo structures and can be used to determine the extension of the systems they belong to; at the same time they give useful hints in revealing the presence of intermediate age stellar populations (see, e.g., the noisy case of the blue galaxy IZw18). Moreover, their emission in the Infra-Red (IR) band has strong consequences in determining the integrated colors of non resolved populations (about 80% of the IR emission comes in fact from this class of stars) and can be used in determining distances if fainter stars can not be resolved (through, e.g., the period-color-luminosity relation of MIRA stars in K band). Last but not least, AGB stars are important producers of light elements (such as carbon, nitrogen and fluorine) as well as heavy ones, being the production site of the main component of the slow neutron capture process (s-process). In this contribution, we will focus on this latter aspect.

Key words. Stars: evolution – Stars: AGB and post-AGB – Stars: abundances

1. Introduction

During the AGB phase, the stellar structure consists of a partially degenerate carbon-oxygen core, an He shell, separated from an H shell by the He-intershell region, and by a convective envelope. The energy required to supply the surface irradiation is mainly provided by the H burning shell, located just below the inner border of the envelope. This situation is recurrently interrupted by the devel-

opment of thermonuclear runaways (Thermal Pulses, TPs), driven by violent He-burning ignitions (3α reactions). As a consequence of a TP, the He-intershell becomes unstable against convection for a short period, because the 3α timescale is locally shorter than the thermodynamic timescale the structure need to expand these regions. Then, the external layers are pushed outwards (and therefore cooled) and, later on, the H shell temporarily dies down. In the He-intershell, He is partially converted into carbon. During the AGB phase, the main neutron sources is the ^{13}C(a,n)^{16}O reaction, active in radiative conditions during the interpulse period; an additional neutron burst comes from the ^{22}Ne(a,n)^{25}Mg reaction, which is marginally activated within the convective shell originated by the TP. In order to obtain a sufficient amount of ^{13}C, a diffusion of protons from the H-rich envelope into the C-rich radiative zone is needed: the diffused proton are captured from the abundant ^{12}C present in the intershell via the ^{12}C(p,γ)^{13}N($\beta^-\nu$)^{13}C nuclear chain, leading to the formation of a tiny ^{13}C-pocket. When in this region the temperature reaches about 10^8 K, the ^{13}C(a,n)^{16}O reaction results efficiently activated and produces a large amount of neutrons, leading to the s-process nucleosynthesis.

2. The FRANEC code

Models presented in this work have been calculated by means of the FRANEC stellar evolutionary code (Chieffi et al. 1998). A major improvement in our code has been the introduction of a physical algorithm for the treatment of the convective/radiative interface at the inner border of the convective envelope (Straniero et al. 2006), whose principal by-product is the formation of a tiny ^{13}C pocket after each TDU episode. In Fig.1 we report mass fractions of selected isotopes in the 3^{rd} ^{13}C pocket for a 2 $M_\odot$ model with solar metallicity. The ^{13}C pocket (solid line) partially overlaps with a more external ^{14}N pocket (long-dashed line); the maximum of the ^{14}N coincides with the region where the protons diffused from the convective envelope at the epoch of the TDU were abundant enough to convert almost all

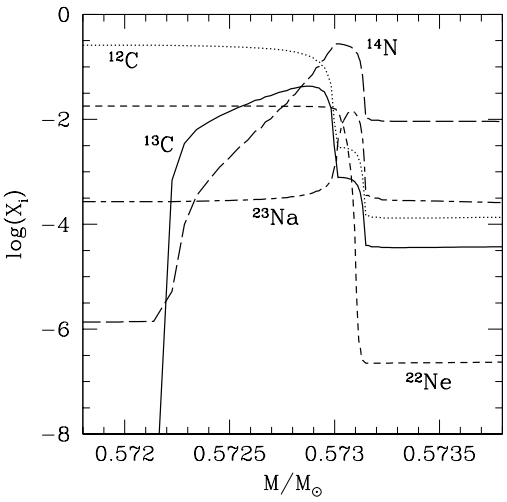

Fig. 1. Mass fractions of selected isotopes in the third ^{13}C pocket of a 2 $M_\odot$ model with solar metallicity. Other two pockets are clearly identified: the ^{14}N and the ^{23}Na pockets.

^{13}C to ^{14}N by proton capture. This is also the region where the ^{23}Na (short-dashed-long-dashed line) has been efficiently produced by the ^{22}Ne(p,γ)^{23}Na reaction. The extension in mass of the first ^{13}C-pockets is about ($6\div7 \times 10^{-4}$ $M_\odot$) and then decreases pulse after pulse down to $2 \times 10^{-4} M_\odot$, following the shrinking of the He-intershell region.

The simultaneous solution of the stellar structure equations and of the full nucleosynthesis network including all the relevant isotopes up to the termination point of the s-process path (Pb-Bi) requires a relevant computational power. This coupling has not been feasible so far, but this limitation has been overcome thanks to the last generation of computers and to the adoption of smart algorithms to invert sparse matrixes of huge size. AGB models presented in this work have been calculated by using an extended set of nuclear processes including all chemical species involved in the s-process nucleosynthesis (Straniero et al. 2006): this network is continuously upgraded according to the latest theoretical and experimental nuclear physics improvements.

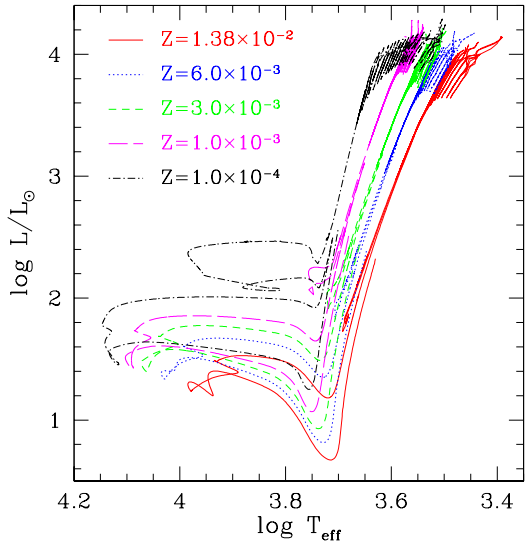

Fig. 2. Evolutionary tracks in the HR diagram of the five 2 $M_\odot$ models. See text for details.

Finally, these models benefit of another important improvement, whose effects are particularly important at low metallicities: the introduction of C-enhanced low temperature opacities. In the atmosphere of an AGB star, C dredge-up substantially affects the molecular contribution to the opacity for temperatures lower than 4000 K (Marigo 2002). Therefore, in order to overcome this limitation, we constructed low temperature C- and N-enhanced opacity tables, suitable for AGB model calculations: the new AGB models succeed in reproducing the photometric and spectroscopic properties of their observational counterparts (Cristallo et al. 2007).

3. Results

In this Section, we present a recent set of low mass AGB models (M=2$M_\odot$) spanning a large range of metallicity (Cristallo et al., in preparation): Z=1.38×10^{-2} (corresponding to the initial solar metallicity), Z=6.0×10^{-3}, Z=3.0×10^{-3}, Z=1.0×10^{-3} and Z=1.0×10^{-4}. In Fig.2 we report the HR diagram of these five models. Note the upper region of the plot, where the AGB phase of the models clearly show the effects of using C-enhanced molecular opacities: during this phase, models show in fact reductions up to a factor 2 of the surface temperature. This feature has never been evidenced when using solar-scaled molecular opacities.

In Fig.3 we report the final surface chemical distributions obtained for Z=1.38×10^{-2} (blue dotted curve), Z=3.0×10^{-3} (red long-dashed curve) and Z=1.0×10^{-4} (dark solid curve). The final C/O envelope ratio in the solar metallicity model is 1.88, while it becomes larger than 1 when the core mass is about 0.6 $M_\odot$ and the bolometric magnitude is about −5.0 mag, in good agreement with the Galactic C-star luminosity function (Guendalini et al. 2006). The abundance of Sr, Y and Zr at the first s peak, the so-called ls elements (*light* s elements), is comparable with the one of the hs elements (*heavy* s elements) Ba, La, Ce, Pr, Nd at the second s peak. Lead is under-produced with respect to barium. The [hs/ls] attained in the envelope when C/O=1 is in good agreement with those measured in galactic C(N) Giants (Abia et al. 2002). At Z=3×10^{-3} the s-process distribution is peaked around the hs elements. We also obtain an increase in the relative production of carbon and fluorine: this is

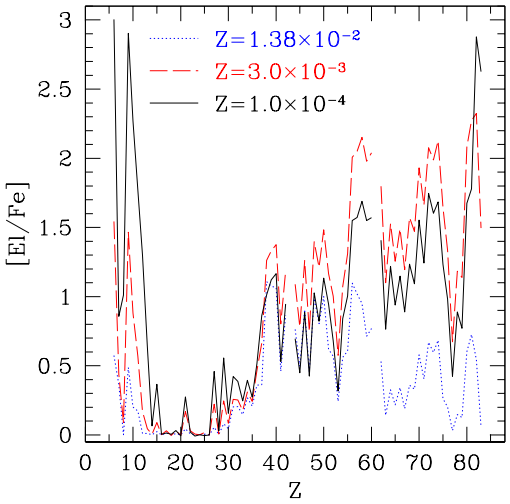

Fig. 3. The final surface composition of three selected evolutionary sequences with different Z.

a direct consequences of the greater efficiency of the TDU episodes. Moreover, let us note that at this metallicity the production of lead (mainly ^{208}Pb) starts being very efficient. At low metallicities, most of the seeds are converted into ^{208}Pb, at the termination point of the s-process fluency (see, e.g., Delaude et al. 2006). Trends illustrated in Fig.3 confirm the previous sentence: a consistent lead production (Z=82) is in fact found. As already stressed before, the lower the metallicity is, the larger the surface carbon is ([C/Fe]~3.0 at Z=10^{-4}). It has to be noted that low metallicity stars enriched in s-process elements show consistent enhancements in the hs region, spanning over a large range (0.8<[hs/Fe]<2.3): even if our final [hs/Fe] value lays within the observed range, we cannot reproduce the observed spread with a single evolutionary model.

3.1. Very low metallicity models

Finally, let us stress that, when dealing with very very metal poor AGBs, the standard AGB evolution scenario is no more valid. In fact, for a given metallicity, there exists a lower mass limit for which a normal TP-AGB phase develops (Cristallo et al. 2007), while stars with smaller initial mass experience a protons engulfment episode during the first fully developed TP (see ,e.g., Iwamoto et al. 2004; Straniero et al. 2004). This occurrence leads to a peculiar s-process nucleosynthesis, a low ^{12}C/^{13}C and a significant synthesis of primary ^{14}N. This new set of very low metallicity models, that represents the current frontier of AGB modeling, is still under analysis (Cristallo et al., in preparation). Main problems found in calculating these models are connected to the choice of the mass loss law, the presence of an oxygen enhancement, the adopted mixing scheme and the nuclear cross section of unstable isotopes far from the β stability valley.

4. Conclusions

In this paper we presented a set of evolutionary models of low mass stars at different metallicities (from solar down to Z=10^{-4}). Recent implementations to the code have been reported and described. Finally, AGB evolution at very low metallicities has been introduced: a comprehensive description of the anomalous behavior of the first fully developed TP in very low metallicity AGB stars will be treated in a future paper.

Acknowledgements. R.G. for the Italian MIUR-PRIN06 Project “Late phases of Stellar Evolution: Nucleosynthesis in Supernovae, AGB stars, Planetary Nebulae”.

References

Abia C., et al., 2002, ApJ, 579, 817
Chieffi, A., Limongi, M., & Straniero, O., 1998, ApJ, 502, 737
Cristallo, S., et al., 2007, ApJ, 667, 489
Delaude, D., et al., 2006, ESO Astrophysics Symposia, edited by Springer-Verlag, pp. 126
Gallino, R., et al., 1998, ApJ, 497, 388
Guandalini, R., et al., 2006, A&A, 445, 1069
Iwamoto, N., et al., 2004, ApJ, 602, 377
Marigo, P., 2002, A&A, 387, 507
Straniero, O., et al., 2004, Mem. SAIt, 75, 665
Straniero, O., Gallino, R., & Cristallo, S., 2006, Nucl.Phys.A, 777, 311